Evaluation of ductile failure models in Sheet Metal Forming

Rui Amaral[1,a], Pedro Teixeira[2], Erfan Azinpour[2], Abel D. Santos[2], J. Cesar de Sa[2]

[1]*INEGI, Institute of Science and Innovation in Mechanical and Industrial Engineering, R. Dr. Roberto Frias 400, 4200-465 Porto, Portugal*
[2]*FEUP, Faculty of Engineering, University of Porto, R. Dr. Roberto Frias, 4200-465 Porto, Portugal*

Abstract. Traditionally, combination of equivalent plastic strain and stress triaxiality parameters are taken into account when performing characterization of material ductility. Some well-established models like Lemaitre model, GTN based models and many others perform relatively well at high-triaxiality stress states but fail to give adequate answers to low-triaxiality states. In this work, three damage models are presented, applied and assessed to a cross-shaped component. Concerning material, AA5182-O, corresponding damage parameters are characterized by an inverse analysis procedure for each damage model.

1 Introduction

When manufacturing automotive body structures, sheet metal forming processes are commonly used, which include drawing, bending and stamping. During this processing the sheet metal can be subjected to large localized deformations with significant through-thickness necking in which 3D stress states develop and dictate the fracture event of the metal blank.

The use of numerical methods such as the finite-element method to handle large plastic deformations has created the possibility to analyse, with a relative success, a forming process during its development stage, including damage and fracture [1].

New generation materials used in automobile industry, as a need to face environmental restrictions (low exhaust emissions) without compromising and even improving safety specifications, are hampered by their lower ductility leading to premature fracture and by the difficulties in predicting such behaviour, thus challenging numerical simulations.

In this paper three damage models are used: Lemaitre's ductile damage model, GTN Gurson-Tvergaard-Needleman (GTN) model, which is an extended version of the model proposed by Gurson [2] and Johnson-Cook model. In the framework of Continuous Damage Mechanics, a local damage model is implemented in Abaqus/Explicit code [3] and corresponding constitutive equations for the coupled model were developed and implemented. It is based on the Lemaitre's ductile damage evolution law, fully coupled with Hill's orthotropic plasticity criterion. Lemaitre model is implemented in a user material subroutine, which was developed to work in the FE package Abaqus. The GTN and Johnson-Cook models were already implemented in FE package, but corresponding damage parameters were identified by current research.

The selected sheet material is an aluminium alloy, AA5182-O. Corresponding characterization for damage parameters is performed by an inverse analysis procedure, using reference experimental tests.

Numerical simulations are presented and the corresponding results are compared with an experimental failure obtained for a cross-shaped component, in order to test and validate the different damage models and their ability for prediction of damage growth and fracture initiation.

2 Damage models

2.1 Lemaitre Damage Model

Induced by large plastic flow, the internal deterioration of the material, which may lead to macroscopic collapse, accompanies the deformation process and therefore, although different in nature, the two dissipative processes influence each other and should, therefore, be coupled at the constitutive level. The model formulated by Lemaitre [4] defines the damage variable as the neat area of a unit surface cut by a given plane corrected for the presence of existing cracks and cavities. By assuming homogenous distribution of micro-voids and the hypothesis of strain equivalence, the effective stress tensor can be represented as:

$$\tilde{\boldsymbol{\sigma}} = \frac{\boldsymbol{\sigma}}{1 - D} \tag{1}$$

where is $\boldsymbol{\sigma}$ the Cauchy stress tensor. The damage variable D value lies between 0 (undamaged state) and 1 (rupture). The evolution law for the internal variables are derived

[a] Corresponding author: ramaral @inegi.up.pt

from a potential of dissipation and considering the damage value, it can be written as:

$$\dot{D} = \frac{\dot{\gamma}}{1-D}\left(\frac{-Y}{S}\right)^{s} \quad (2)$$

where $\dot{\gamma}$ is the plastic consistency parameter and Y is damage energy release rate given by:

$$Y = -\frac{1}{2E(1-D)^2}[(1-\upsilon)\boldsymbol{\sigma}:\boldsymbol{\sigma} - \upsilon(tr\,\boldsymbol{\sigma})^2] \quad (3)$$

where E and υ are the Young's modulus and Poisson's ratio, respectively.

2.2 GTN Damage Model

Based on a micromechanical approach, Gurson [2] has proposed an internal variable to describe material degradation, which represents the volume fraction of micro-cavities that nucleate, grow and coalesce during loading. The original model was further extended by Tvergaard [5] and Needleman [6] replacing the original internal variable f by a modified parameter f^* in order to take into account the accelerated void coalescence process after a critical void volume fraction f_c is reached. The yield function of the GTN damage model is given by:

$$\phi = \left(\frac{\bar{\sigma}}{\sigma_Y}\right)^2 + 2q_1 f^* cosh\left(\frac{3}{2}q_2\frac{\sigma_H}{\bar{\sigma}}\right) - \left(1+q_3 f^{*2}\right) \quad (4)$$

where q_1, q_2 and q_3 are the model parameters, σ_Y the flow stress and σ_H and $\bar{\sigma}$ the hydrostatic stress and equivalent von Mises stress, respectively. The modified porosity parameter f^* is calculated by:

$$f^* = \begin{cases} f & f \le f_c \\ f_c + \dfrac{1/q_1 - f_c}{f_F - f_c}(f - f_c) & f > f_c \end{cases} \quad (5)$$

The evolution law of the void volume fraction is given by:

$$\dot{f} = \dot{f}_G + \dot{f}_N \quad (6)$$

accounting for void growth $\dot{f}_G$ and nucleation $\dot{f}_N$, both variables expressed by:

$$\dot{f}_G = (1-f)tr\,\dot{\boldsymbol{\varepsilon}}_{\boldsymbol{p}} \quad (7)$$

$$\dot{f}_N = \frac{f_N}{S_N\sqrt{2\pi}} exp\left[-\frac{1}{2}\left(\frac{\bar{\varepsilon}_p - \varepsilon_N}{S_N}\right)^2\right]\dot{\varepsilon}_p \quad (8)$$

where f_N, S_N and ε_N are material parameters and $\dot{\boldsymbol{\varepsilon}}_{\boldsymbol{p}}$ is the plastic strain rate tensor.

2.3 Johnson-Cook model

Damage indicators that can express the material's degradation under plastic straining are widely used in industry due to their relative simplicity. These models are often calculated using a fully uncoupled approach, meaning that the progressive degradation does not affect the plastic behaviour of the material. The most used model is the one proposed by Johnson and Cook [7], which, besides the postulation of a phenomenological strain rate and temperature dependent hardening law, have also defined the fracture strain ε_f as a function of stress triaxiality η, plastic strain rate $\dot{\varepsilon}_p$ and temperature θ as:

$$\varepsilon_f = (d_1 + d_2 e^{d_3\eta})\left[1 + d_4 ln\left(\frac{\dot{\varepsilon}_p}{\dot{\varepsilon}_0}\right)\right](1 + d_5\theta) \quad (9)$$

where d_1, d_2, d_3, d_4 and d_5 are material parameters. The corresponding damage indicator is calculated by the expression:

$$D = \sum \frac{\Delta\bar{\varepsilon}_p}{\varepsilon_f} \quad (10)$$

where $\Delta\bar{\varepsilon}_p$ is the equivalent plastic strain increment.

3 Material and damage parameters

3.1 Material characterization

In this article, a mechanical characterization of the aluminium alloy AA5182-O, with 1 mm thickness, was performed [8]. Tensile tests of AA5182-O specimens were conducted for different angles according to the rolling direction. Also monotonic simple shear tests were performed for different angles. The corresponding flow curves are shown in figure 1 and 2.

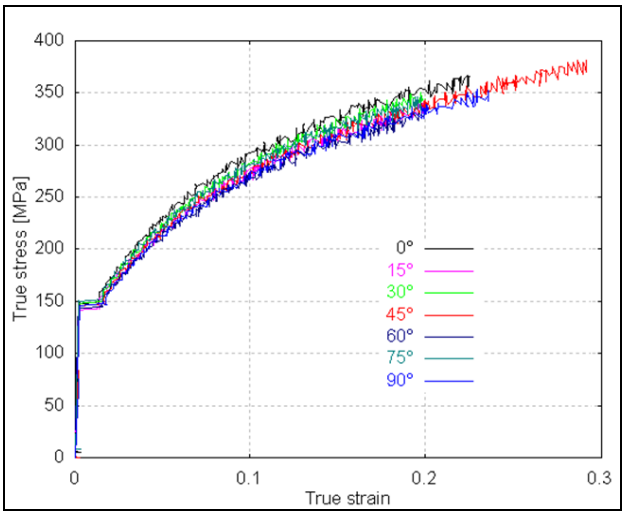

Figure 1. Flow stress-strain curve obtained from uniaxial tensile test for AA5182-O, according to different directions relative to the rolling direction [8].

The fundamental properties of the material obtained from stress-strain curves, such as Young modulus (E), Poisson coefficient (ν), yield stress (Rp), ultimate tensile strength (R_m) and total elongation (e_t), are presented in table 1, as well as the anisotropy coefficients (*r-value*) for different directions relative to rolling direction.

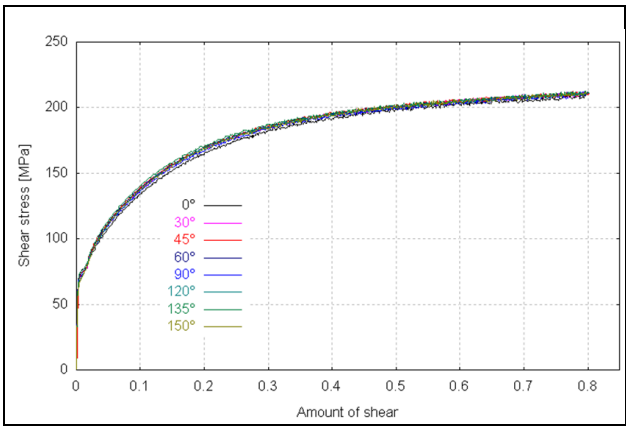

Figure 2. Flow curve obtained from monotonic simple shear test for AA5182-O, according to different directions relative to the rolling direction [8].

Table 1. Mechanical properties for AA5182-O.

Property	Value
Young modulus [GPa]	69
Poisson coefficient	0.3
Yield stress [MPa]	149.5
Ultimate tensile strength [MPa]	283.8
Total elongation [%]	24.4
r_0, r_{45}, r_{90}	0.79, 0.85, 0.7

The behaviour of the aluminium alloy AA5182-O can be well described by using an isotropic hardening given by the Voce Law. Table 2 gives the corresponding parameters obtained for this constitutive model.

Table 2. Voce Law parameters for AA5182-O.

Voce Law $Y = Y_0 + R_{sat}\left[1 - \exp\left(-C_r \cdot \bar{\varepsilon}^p\right)\right]$	
Parameter	**Value**
Y0 [MPa]	149
Rsat [MPa]	208.7
Cr	12.1

3.2 Damage parameter identification

Parameters for presented damage models (section 2), were determined by an inverse numerical analysis based on optimization algorithms. Due to the fact that an inhomogeneous state is prevalent during material softening, experimental and numerical force-elongation curves are considered [9]. The minimization of the mean square error (MSE) between experimental and numerical data is calculated using an optimization algorithm implemented on MATLAB. As a result of the iterative optimization procedure, the best fit values for the presented damage models are obtained. The used methodology is shown in figure 3.

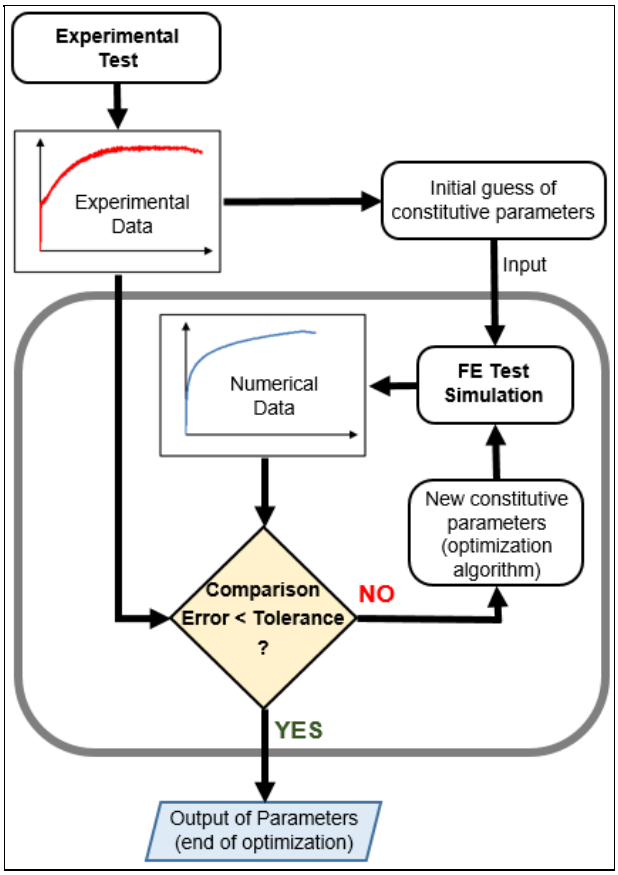

Figure 3. Methodology used for the identification of the damage parameters.

Lemaitre damage model parameters have been identified based on the results obtained from the tensile test [10]. The parameters for Lemaitre damage model are presented in table 3.

Table 3. Lemaitre damage model parameters for AA5182-O.

Parameter	Value
Damage Exponent - s	1.0
Damage Denominator – S [MPa]	1.25

The GTN damage model has 7 parameters that characterize the behaviour of the material, but there is a mutual dependency that must be considered [11]. According to literature, the parameters q_1, q_2 and S_N are kept constant [12, 13] and the initial void volume fraction f_0 can be obtained through an analytic expression based on chemical composition [14], which means that finally only 4 parameters will be determined. In table 4 the parameters of GTN damage model are presented, obtained from the identification procedure and using the experimental uniaxial tensile and biaxial bulge test.

Table 4. GTN damage model parameters for AA5182-O.

Parameter	q_1	q_2	q_3	f_0	f_C	f_F	ε_N	S_N	f_N
Value	1.5	1	2.25	0.01	0.021	0.04	0.3	0.1	0.001

The Johnson-Cook damage model is employed without strain rate and temperature effects, which means that parameters d_4 and d_5 are not considered. Since this model accumulates failure, in which the failure strain is more dependent to stress triaxiality than the others variables, it is more important the determination of parameters d_1, d_2 and d_3 [15]. In table 5 the parameters of Johnson-Cook damage model are presented, obtained from the identification procedure and using uniaxial tensile and simple shear test. The obtained parameters are similar to those identified by Sun *et al* [16], also for AA5182-O.

Table 5. Johnson-Cook damage model parameters for AA5182-O.

Parameter	**Value**
d_1	0.024
d_2	0.38
d_3	1.5
d_4, d_5	0

4. Results and discussion

4.1 Cross Tool geometry

The applicability of the described damage models is illustrated by means of an experimental deep drawing failure case of a cross-shaped (figure 4) sheet metal component [17].

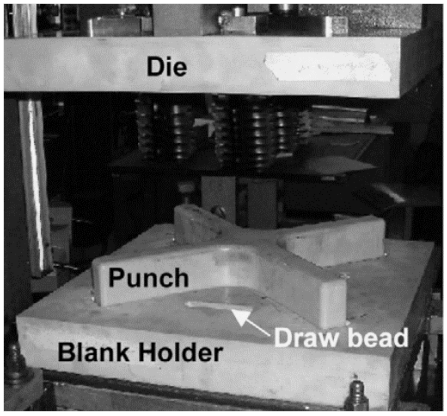

Figure 4. Tool geometry and active parts. The punch cross geometry has 487 mm length.

Using an aluminium alloy AA5182-O sheet with a thickness of 1 mm, failure occurs as shown in figure 5.

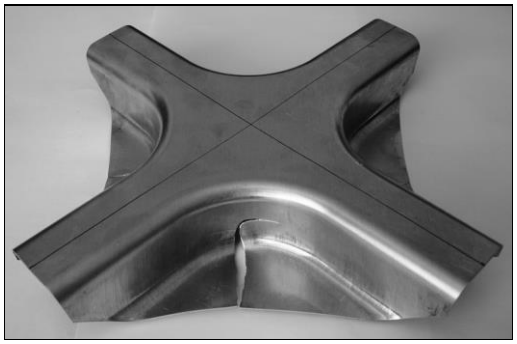

Figure 5. Cross-shaped component with breakage.

4.2 Numerical model

A 3D FEM explicit analysis (Abaqus/Explicit) model is considered with one quarter of the real setup, due to symmetry. The tools are modeled as fully rigid surfaces with discretization performed by three noded rigid elements (R3D3 type from Abaqus Library). The blank discretization uses a double layer of deformable eight noded solid elements with reduced integration (C3D8R type from Abaqus Library), making a total of 1186 elements. Regarding the material behaviour, the blank was modeled as an elasto-plastic material with isotropic hardening described by Voce Law. The blank material properties used, were already presented in section 3. The GTN and Johnson-Cook models are implemented in FE package Abaqus, but in the case of Lemaitre model a user material subroutine was developed and implemented in the same FE program.

4.3 Results

Figures 6, 7 and 8 present the contours of the equivalent plastic strain and the damage value for the three considered damage models, respectively, Lemaitre, GTN and Johnson-Cook.

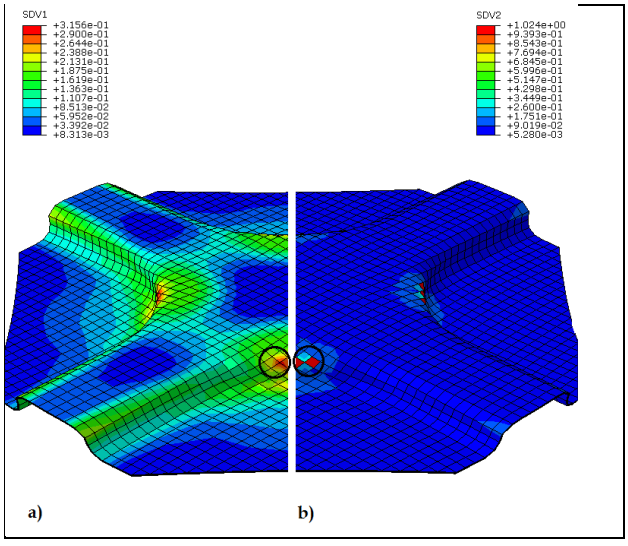

Figure 6. Obtained results using the identified parameters of Lemaitre damage model. a) Equivalent plastic strain; b) Damage contour prediction.

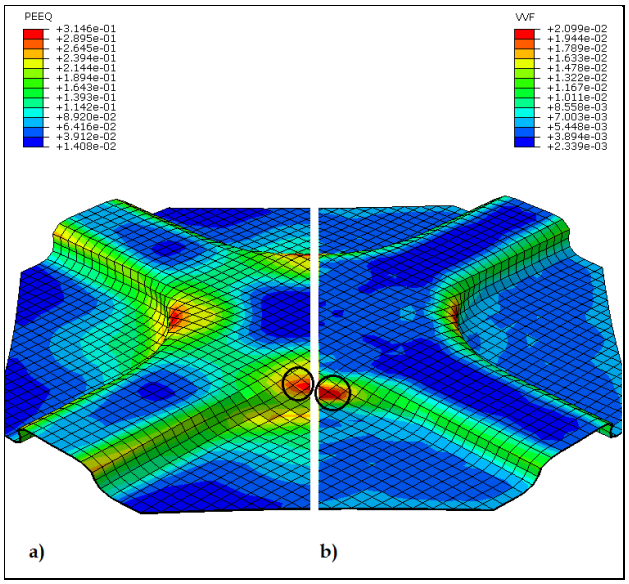

Figure 7. Obtained results using the identified parameters of GTN damage model. a) Equivalent plastic strain; b) Damage contour prediction.

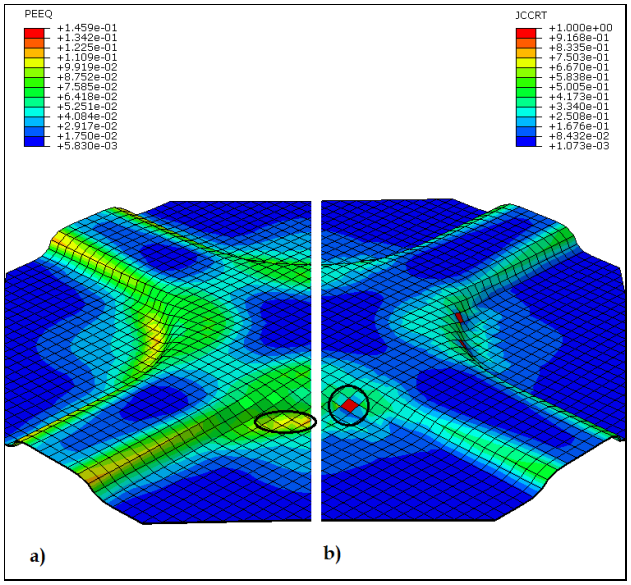

Figure 8. Obtained results using the identified parameters of Johnson-Cook damage model. a) Equivalent plastic strain; b) Damage contour prediction.

The figure 9 shows the levels of triaxiality in the cross-shaped component. Figures 6 to 8 shows the fracture initiation for the damage models presented in this study. For current proposed experimental component, both maximum strain and damage variable have very close locations (at the vertical wall of cross-center geometry). Usually, when analyzing fracture location, maximum damage is attained in regions where triaxiality is higher. All damage models in this study show similar trend, which is in accordance with experimental evidence. However the punch displacement to failure and maximum strain are different.

Although Lemaitre and GTN models predict fracture initiation at the same punch displacement, Johnson-Cook predicts failure at lower punch displacement and lower plastic strain. This difference can be attributed to inexistence (not considered) of plastic softening modeling in Johnson-Cook model, while the other models include such softening.

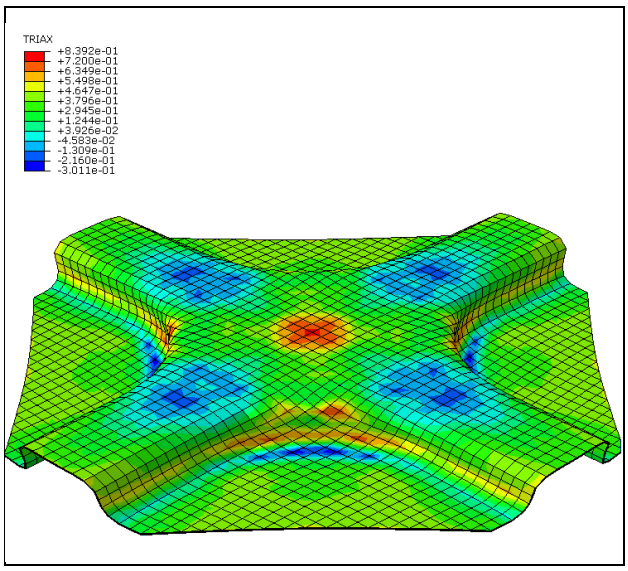

Figure 9. Triaxiality levels present in cross-shaped component.

Another reason can be due to the parameter identification basis for each model, which in turn is related with triaxiality values. The tests used for Johnson-Cook parameter identification are related with low triaxiality tests (shear+tensile), although in case of GTN and Lemaitre, the tests used have higher triaxiality values (tensile+bulge). Since experimental component shows critical deformation localization for higher triaxialities, this means that GTN and Lemaitre and corresponding damage parameters are more adjusted to predict failure in this component, which is in accordance to obtained numerical results and experimental evidence.

5 Conclusions

In this paper, three different ductile damage models, GTN, Johnson-Cook and Lemaitre were described and compared for prediction of damage in sheet metal forming processes. A finite element analysis of a cross-shaped component, using the parameters obtained for the aluminum alloy AA5182-O, has been taken as a basis of comparison between the damage models, in order to assess the accuracy of the results. For this particularly case, the simulations of GTN and Lemaitre show a good agreement with the damage location observed in the experimental component. The parameters obtained for the Johnson-Cook damage model, from tensile and simple shear tests, overestimate the development of damage at high triaxialities.

It is known that to cover the range of the relation between stress triaxiality and strain at failure, namely on low stress triaxiality states, other failure models are needed [18, 19] and therefore they will be tested in future studies.

Acknowledgements

The authors gratefully acknowledge the financial support of the Portuguese Foundation for Science and Technology (FCT) under project PTDC/EMS-TEC/6400/2014.

References

1. P. Teixeira, A.D. Santos, J.M.A. César de Sá, F.M. Andrade Pires, A. Barata da Rocha. Int. J. Mat. Form., 2, 463-466, (2009)
2. L. Gurson. J. Eng. Mat. Tech., 99, 2–15, (1977)
3. P. Teixeira, A.D. Santos, F.M. Andrade Pires, J. César de Sá. J. Mat. Proc. Tech., **177**, 278-281, (2006)
4. J. Lemaitre. J. Eng. Mat. Tech, 107, 83-89, (1985)
5. V. Tvergaard V. Int. J. Fract, 18, 237-252, (1982)
6. Needleman, V. Tvergaard. Acta metall., **32**, 157-169, (1984)
7. G. R. Johnson, W. H. Cook. Eng. Fract. Mech., **21**, 31-48, (1985)
8. 3DS report, 2001. Selection and identification of elastoplastic models for the materials used in the benchmarks. 18-Months Progress Report, Inter-regional IMS contract ‘‘Digital Die Design Systems (3DS)’’, IMS 1999 000051
9. Tsoupis, M. Merklein. 13th LS-Dyna Conf., (2013)
10. Lemaitre, R. Desmorat, *Engineering Damage Mechanics*, (2005)
11. D.A. Wang, W.Y. Chien, K.C. Liao, S.C. Tang, Ch. J. Mech Series A **19**, 161-168, (2003)
12. Z.L. Zang, Fatig. Fract. Eng. Mat. Struct 19, 561-570, (1996)
13. D.Z. Sun, A. Hönig, W. Böhme, W. Schmitt. Frac. Mec. **25**, 343-357, (1995)
14. M. Doing, K. Roll. AIP Conf., 1541-1546, (2011)
15. Marzbanrad, S. Noruzi, A. Ahmado, S.K. ISME2013, (2013).
16. H.T. Sun, J. Wang, G.Z. Shen, P. Hu. Int. J. Auto. Tech. 14, 605-610, (2013)
17. Pinto, A.D. Santos, P. Teixeira, P.J. Bolt. J. Nat. Proc. Tech., **202**, 47-53, (2008)
18. L. Malcher, F.M. Andrade Pires , J.M.A. César de Sá, Int. J. Plast, **30–31**, 81–115, (2012)
19. L. Malcher , F.M. Andrade Pires, J.M.A. César de Sá, Int. J. Plast., **54**, 193–228, (2014)